Copper chaperone for superoxide dismutase is essential to activate mammalian Cu/Zn superoxide dismutase

Philip C. Wong*†, Darrel Waggoner‡, Jamuna R. Subramaniam*, Lino Tessarollo§, Thomas B. Bartnikas‡, Valeria C. Culotta¶, Donald L. Price*‖, Jeffrey Rothstein‖**, and Jonathan D. Gitlin‡**

Departments of *Pathology, ‖Neurology and **Neuroscience, The Johns Hopkins University School of Medicine, and ¶Department of Environmental Health Sciences, The Johns Hopkins University School of Public Health, Baltimore, MD 21205; ‡Department of Pediatrics, Washington University School of Medicine, St. Louis, MO 63110; and §Advanced BioScience Laboratories–Basic Research Program, National Cancer Institute–Frederick Cancer Research and Development Center, Frederick, MD 21702

Edited by Solomon H. Snyder, Johns Hopkins University School of Medicine, Baltimore, MD, and approved December 27, 1999 (received for review October 25, 1999)

Recent studies in *Saccharomyces cerevisiae* suggest that the delivery of copper to Cu/Zn superoxide dismutase (SOD1) is mediated by a cytosolic protein termed the copper chaperone for superoxide dismutase (CCS). To determine the role of CCS in mammalian copper homeostasis, we generated mice with targeted disruption of *CCS* alleles ($CCS^{-/-}$ mice). Although $CCS^{-/-}$ mice are viable and possess normal levels of SOD1 protein, they reveal marked reductions in SOD1 activity when compared with control littermates. Metabolic labeling with ^{64}Cu demonstrated that the reduction of SOD1 activity in $CCS^{-/-}$ mice is the direct result of impaired Cu incorporation into SOD1 and that this effect was specific because no abnormalities were observed in Cu uptake, distribution, or incorporation into other cuproenzymes. Consistent with this loss of SOD1 activity, $CCS^{-/-}$ mice showed increased sensitivity to paraquat and reduced female fertility, phenotypes that are characteristic of SOD1-deficient mice. These results demonstrate the essential role of any mammalian copper chaperone and have important implications for the development of novel therapeutic strategies in familial amyotrophic lateral sclerosis.

A number of genetic studies in *Saccharomyces cerevisiae* have indicated that the delivery of Cu to specific intracellular pathways is mediated by a family of intracellular proteins termed copper chaperones (1, 2). Human homologues for several of these chaperones have been identified, and in the case of Cu/Zn superoxide dismutase (SOD1), both the yeast and human copper chaperone for superoxide dismutase (CCS) were found to be essential for the activation of yeast SOD1 (3). CCS directly interacts with SOD1 (4, 5), and both proteins colocalize within multiple cell types including motor neurons (6). Biochemical analysis demonstrates that yeast CCS is sufficient to incorporate Cu into SOD1 through direct transfer under restricted concentrations of intracellular free Cu. Moreover, structural and functional studies of yeast CCS indicate that this is accomplished by a complex intermolecular reaction involving a unique domain structure of the CCS molecule (7, 8).

Despite these findings, there is currently no evidence indicating an essential role for any metallochaperone in mammalian Cu trafficking or homeostasis. This issue is particularly important with regard to SOD1 given the importance of this enzyme in antioxidant defense and compelling evidence supporting the view that mutations in SOD1 cause familial ALS through a gain of toxic property (9–11). Although the molecular mechanisms whereby mutant SOD1 causes selective motor neuron death remain uncertain, recent data suggest a direct role for copper through conformational changes in mutant SOD1 to facilitate the interactions of the catalytic Cu with small molecules such as peroxynitrite (12) or hydrogen peroxide (13) to generate toxic free radicals that damage essential constituents of motor neurons. Because CCS has been shown to interact with both wild-type and familial amyotrophic lateral sclerosis (FALS)-linked mutant SOD1 (4) and copper incorporation into these molecules in yeast is CCS dependent (14), we have now directly examined the role of mammalian CCS in SOD1 copper incorporation with the realization that such a model may have direct implications for our understanding of the pathogenesis of motor neuron degeneration in FALS.

Materials and Methods

Gene Targeting Vector and Embryonic Stem (ES) Cells. To target the CCS gene in ES cells, CCS genomic clones were isolated from a 129/Sv strain of mouse (Lambda FIX II Library, Stratagene) as previously described (13) by using a mouse CCS cDNA as probe. We replaced a 2.5-kb *Xho*I/*Bam*HI fragment containing the first two coding exons with the *neo* gene under the control of the PGK promoter. Introduction of a negative selection marker, the herpes simplex virus thymidine kinase gene, at the 5′ end of the construct allowed the use of the positive and negative selection scheme (14). The targeting vector was linearized at a unique *Sal*I site before transfection into CJ7 ES cells (15), which were subjected to double selection. Clones were picked and expanded, and DNA was isolated from a portion of the cells and screened by Southern blot analysis. Targeted frozen cells were expanded and injected into C57BL/6J blastocysts to produce highly chimeric male mice that transmitted the targeted *CCS* allele in the germline. $CCS^{+/-}$ mice were intercrossed to obtain the $CCS^{-/-}$ animals. Genotypes were determined by PCR amplification of tail DNA. One primer set (5′ ATGGCTTCGAAGTCGGGG; 5′ CCTTTCAGGGTCTTGTGC) was used to detect the endogenous *CCS* locus, and another primer set (5′ CCATTGCTCAGCGGTGCTG; 5′ GCCAAGGAGATGGTATGTATGTATG) was used to detect the targeted *CCS* allele.

SDS/PAGE and Immunoblotting. Mouse tissues were homogenized in buffer containing 20 mM Tris·HCl (pH 7), 1% Triton X-100, 1 mM EDTA, and a protease inhibitor mixture (50 μg/ml leupeptin, 50 μg/ml pepstatin, 10 μg/ml aprotinin, and 0.25 mM phenylmethylsulfonyl fluoride). Protein extracts (20 μg) were fractionated onto a 14% SDS-polyacrylamide gel, electrophoresed, and transferred to polyvinylidene difluoride filters. CCS or SOD1 was detected by using a highly specific CCS (6) or SOD1 polyclonal antibody (16), followed by horseradish peroxidase-conjugated anti-rabbit IgG.

This paper was submitted directly (Track II) to the PNAS office.

Abbreviations: SOD1, Cu/Zn superoxide dismutase; CCS, copper chaperone for superoxide dismutase; FALS, familial amyotrophic lateral sclerosis; ES, embryonic stem.

†To whom reprint requests should be addressed at: Department of Pathology, The Johns Hopkins University School of Medicine, 558 Ross Research Building, 720 Rutland Avenue, Baltimore, Maryland 21205-2196. E-mail: wong@jhmi.edu.

The publication costs of this article were defrayed in part by page charge payment. This article must therefore be hereby marked "*advertisement*" in accordance with 18 U.S.C. §1734 solely to indicate this fact.

Article published online before print: *Proc. Natl. Acad. Sci. USA*, 10.1073/pnas.040461197. Article and publication date are at www.pnas.org/cgi/doi/10.1073/pnas.040461197

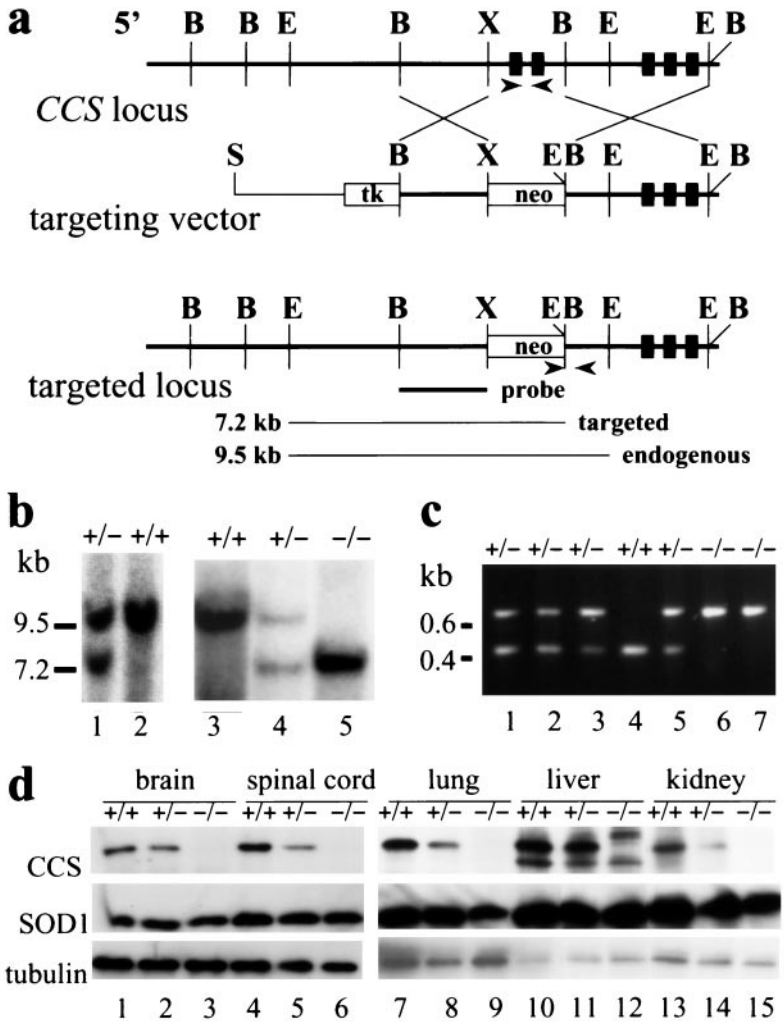

Fig. 1. Targeted disruption of the *CCS* gene by homologous recombination. (*a*) Maps of the wild-type *CCS* allele, the targeting vector, and the targeted *CCS* locus. Exons 1 to 5 of the *CCS* gene are denoted by black boxes. The targeting vector shows the replacement of exons 1and 2 and flanking genomic sequences including portions of the promoter by the neomycin gene (*neo*) and the HSV thymidine kinase gene (*tk*). Lines below indicate expected sizes from a Southern blot for *Eco*RI-digested fragments detected with a 5′-probe (black bar) from targeted and endogenous *CCS* alleles. B, *Bam*HI; E, *Eco*RI; H, *Hin*dIII; S, *Sal*I; X, *Xho*I. Arrows denote the sites within the targeted and wild-type *CCS* locus from which PCR primers were chosen for genotyping. (*b*) Analysis of genomic DNA from ES cells (lanes 1 and 2) and from progeny of $CCS^{+/-}$ crosses (lanes 3–5). Genotypes for the *CCS* targeted allele and the *Eco*RI fragments detected for endogenous (9.5 kb) and targeted (7.2 kb) *CCS* alleles with the 5′ probe are indicated. (*c*) PCR analysis of DNA extracted from tail clips. By using primers indicated in *a*, the 0.4-kb or 0.6-kb fragment is specific to the endogenous or targeted *CCS* allele respectively; wild-type (lane 4), heterozygous (lanes 1, 2, 3, and 5), and homozygous (lanes 6 and 7) *CCS* knockout mice are indicated. (*d*) Protein extracts (20 μg) from various tissues of wild-type (lanes 1, 4, 7, 10, and 13), heterozygous (lanes 2, 5, 8, 11, and 14), and homozygous (lanes 3, 6, 9, 12, and 15) *CCS* knockout mice were immunoblotted by using antisera specific for CCS, SOD1, and α-tubulin. Bound antibodies were detected by using an enhanced chemiluminescent detection method.

The immunocomplex was visualized by using the enhanced chemiluminescence method (Amersham).

SOD1 Activity Assays. Mouse tissues were homogenized in buffer containing 20 mM Tris·HCl (pH 7), 1% Triton X-100, 1 mM EDTA, 5 mM bathocuproine sulfonate (Sigma), and a protease inhibitor mixture (50 μg/ml leupeptin, 50 μg/ml pepstatin, 10 μg/ml aprotinin, and 0.25 mM phenylmethylsulfonyl fluoride). After centrifugation at 10,000 $\times$ *g* for 5 min, the supernatant was fractionated on a 7.5% native polyacrylamide gel, and SOD1 activities were determined as previously reported (17).

A cytochrome *c*/xanthine oxidase-based assay was also used to determine SOD1 activities as previously described (18). The tissue lysates were also analyzed in the presence of 1 mM KCN to determine manganese superoxide dismutase (SOD2) activities. The amount of extracellular Cu/Zn superoxide dismutase (SOD3) was determined from analysis of mouse tissues harvested from SOD1 null mice (gift of Y.S. Ho, Wayne State University, Detroit, MI). The SOD1 activity was calculated by subtracting both the SOD2 and SOD3 activities from the total superoxide dismutase activity.

Cu Incorporation Studies in Mice and Fibroblasts. Primary fibroblasts were metabolically labeled with 200 μCi ^{64}Cu for 2 hr. Cell lysates were prepared in 50 mM Hepes (pH 7.6)/250 mM NaCl/0.1% Nonidet P-40/5 mM EDTA, and a protease inhibitor mixture (50 μg/ml leupeptin, 50 μg/ml pepstatin, 10 μg/ml aprotinin, and 0.25 mM phenylmethylsulfonyl fluoride). Protein extracts (50 μg) were fractionated on 10% native-polyacrylamide gel and exposed to PhosphorImager (Molecular Dynamics). Animals were injected with 500 μCi ^{64}Cu intraperitoneally for serum, liver, and kidney homogenates and intrathecally for brain and spinal cord homoge-

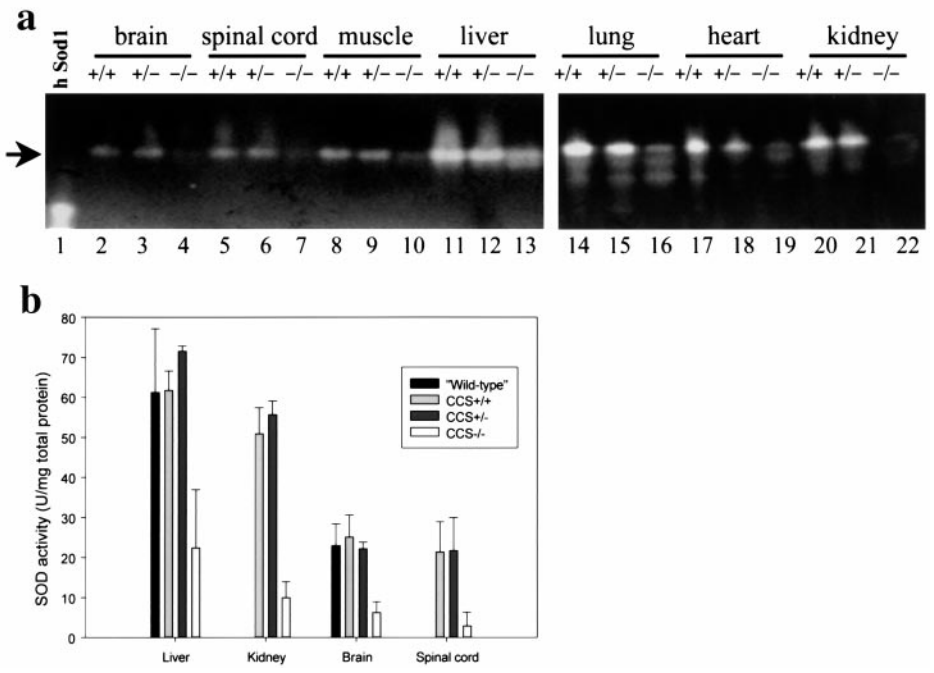

Fig. 2. Diminished SOD1 enzymatic activity in *CCS* knockout mice. (*a*) SOD1 activity assay gel of 25 or 50 μg protein extracts, respectively, from brain, spinal cord, muscle, and liver or from lung, heart, and kidney of wild-type (lanes 2, 5, 8, 11, 14, 17, and 20), heterozygous (lanes 3, 6, 9, 12, 15, 18, and 21), and homozygous (lanes 4, 7, 10, 13, 16, 19, and 22) *CCS* knockout mice. Arrow denote the position of mouse SOD1. Purified human erythrocyte SOD1 is shown in lane 1. (*b*) SOD1 activity determined from tissue extracts indicated by using a cytochrome *c*/xanthine oxidase method. The averages of SOD1 activities $+/-$ standard deviations from three mice for each CCS genotype are shown. ''Wild-type'' values, as previously reported (21), are included for comparison.

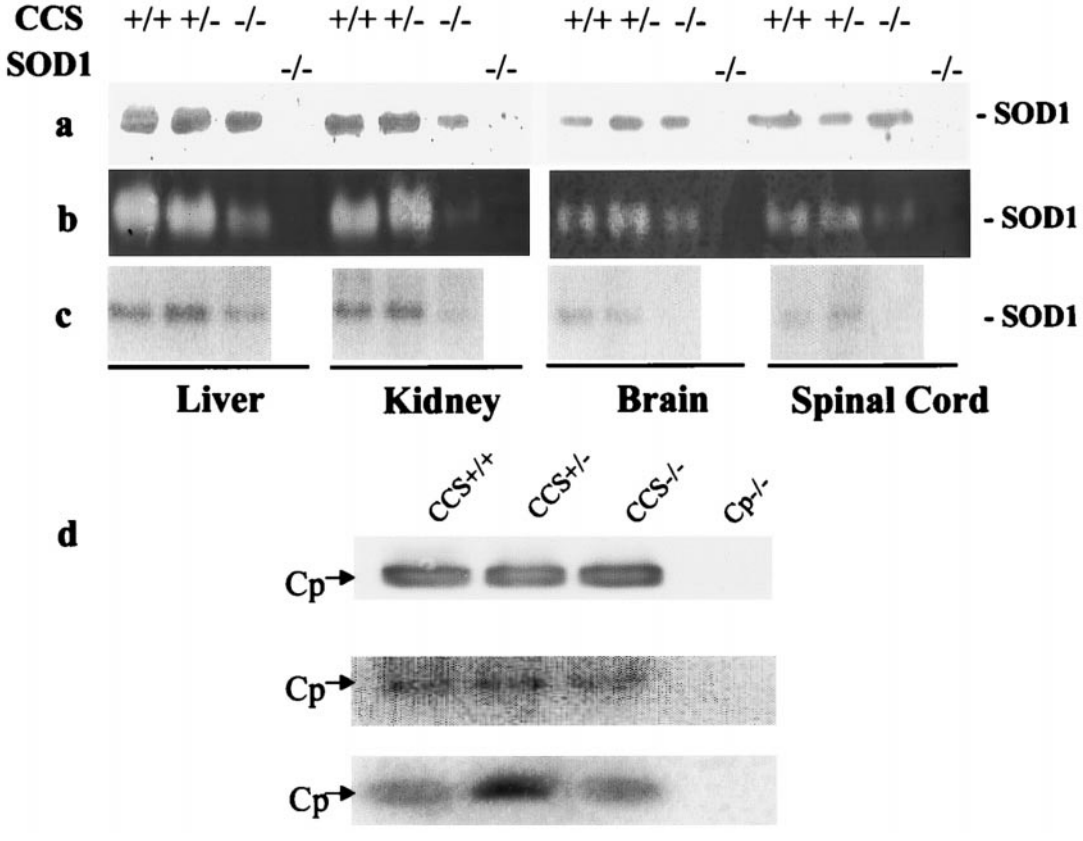

Fig. 3. Copper incorporation into SOD1 is impaired in *CCS* knockout mice. Protein extracts from various tissues of wild-type, heterozygous, and homozygous *CCS* knockout mice and homozygous SOD1 knockout mice were obtained. (*a*) SDS/PAGE gel of liver (50 μg), kidney (75 μg), brain and spinal cord (100 μg), immunoblotted with antisera to SOD1. (*b*) SOD1 gel activity assay on same samples as *a*. (*c*) ^{64}Cu incorporation into SOD1, 100 μg of protein lysate for each tissue. (*d*) Analysis of serum samples from wild-type, heterozygous, and homozygous *CCS* knockout mice and homozygous ceruloplasmin knockout mice. (*Top* to *Bottom*) Immunoblot with antisera to human ceruloplasmin, ^{64}Cu incorporation to ceruloplasmin, and ceruloplasmin activity gel assay.

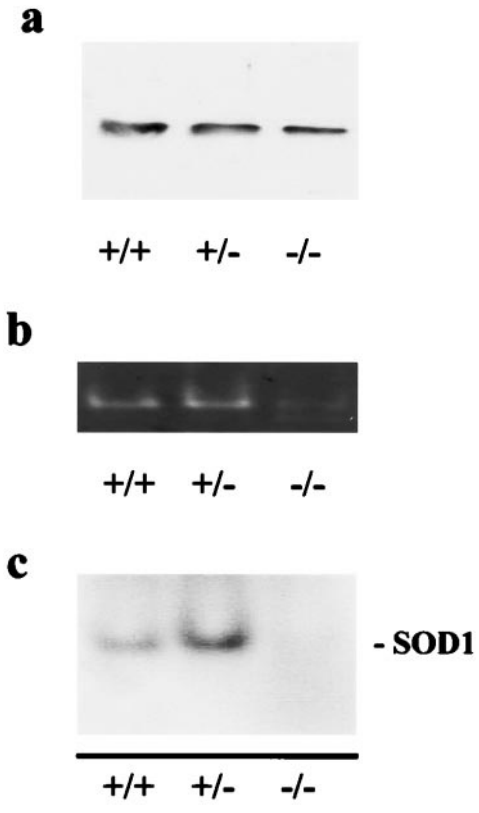

Fig. 4. Decreased copper incorporation into SOD1 is detected in fibroblasts derived from $CCS^{-/-}$ mice. Primary fibroblast cultures were isolated from wild-type, heterozygous, and homozygous *CCS* knockout mice. (*a*) Protein lysates (50 μg) immunoblotted with antisera to SOD1. (*b*) SOD1 gel activity assay of 50 μg protein extract. (*c*) Protein lysate (50 μg) of ^{64}Cu-labeled fibroblasts.

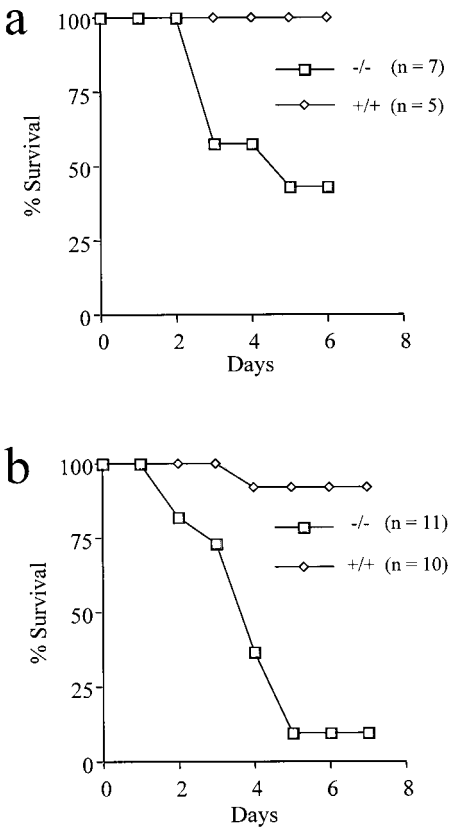

Fig. 5. Increased sensitivity to paraquat in $CCS^{-/-}$ mice. Cumulative probability of survival of age-matched $CCS^{+/+}$ and $CCS^{-/-}$ mice of both genders after exposure of paraquat at a dose of (*a*) 15 ($P < 0.025$) or (*b*) 25 ($P < 0.005$) mg/kg body weight.

nates. Tissues were homogenized in the buffer described above and then treated identically to the fibroblasts.

Paraquat Treatment. Mice receiving a single dose of paraquat by intraperitoneal injection were observed over a period of 1 wk. Lungs and other organs were harvested from affected mice and evaluated histologically.

Histological Analysis. Anesthetized mice were killed by transcardiac perfusion with 0.1 M PBS (pH 7.4), followed by 4% paraformaldehyde in 0.1 M PBS (pH 7.4). Brain, spinal cord, ovary, and other organs were removed and postfixed in the same fixative, embedded in paraffin, sectioned (10 μm), and stained with hematoxylin and eosin, cresyl violet, or luxol fast blue.

Results

Generation of *CCS*-Deficient Mice. We used a homologous recombination strategy in ES cells to inactivate the mouse *CCS* gene. In the *CCS* targeting vector, a 2.5-kb fragment containing the first two exons, part of the promoter, and the first two introns of the *CCS* gene was substituted by a neomycin-resistance gene (Fig. 1*a*). CJ7 ES cells were transfected with the linearized *CCS* targeting vector, and 16 clones were targeted at the *CCS* locus (Fig. 1*b*). *CCS*-targeted ES cells were used to generate the $CCS^{-/-}$ mice. Genotyping of the $CCS^{-/-}$ mice was performed by using DNA blotting (Fig. 1*b*) and PCR methods (Fig. 1*c*). To confirm that the targeting event led to inactivation of the *CCS* gene, protein immunoblotting analysis of brain extracts with a highly specific CCS antibody (6) was performed. In $CCS^{+/-}$ mice, CCS accumulated to ≈50% the level of control littermates for all tissues examined, whereas the same tissues from $CCS^{-/-}$ mice showed no detectable level of CCS (Fig. 1*d*). These results confirm the inactivation of CCS.

CCS Is Essential for SOD1 Enzymatic Activity. To determine whether CCS is essential for SOD1 activity, we examined the enzymatic activity of SOD1 in cell lysates from various tissues of $CCS^{-/-}$ mice by using an activity gel or a solution assay. Compared with lysates from $CCS^{+/-}$ mice or control littermates, lysates from $CCS^{-/-}$ mice revealed a marked reduction of SOD1 activity by using an *in situ* native gel assay (Fig. 2*a*); we estimated that all $CCS^{-/-}$ tissues examined retain 10–20% of normal SOD1 activity with the exception of liver, which is ≈30%. Quantitative SOD1 solution assay revealed similar findings: tissues such as spinal cord, brain, and kidney from $CCS^{-/-}$ mice retained ≈15% of normal SOD1 activity, whereas liver showed a higher level of ≈30% (Fig. 2*b*). However, protein blotting analysis showed that the levels of SOD1 polypeptide from lysates of $CCS^{-/-}$ mice were similar to those of $CCS^{+/-}$ mice or control littermates (Fig. 1*d*). Although these results do not exclude the possibility of another CCS homologue in mammals, they demonstrate that the superoxide scavenging activity in CCS-deficient mice is significantly diminished and establish that CCS is essential to activate SOD1 *in vivo*.

CCS Is Essential to Incorporate Copper into SOD1. To test whether the reduced SOD1 activity observed in CCS-deficient mice is caused by an abnormality in copper incorporation into SOD1 polypeptide, *in vivo* ^{64}Cu metabolic labeling analyses were performed in CCS-deficient mice as well as in fibroblast cells derived from these mice. As expected, in control mice or $CCS^{+/-}$ mice that received ^{64}Cu injections, we observed ^{64}Cu-labeled proteins corresponding to SOD1 in lysates from spinal cord, brain,

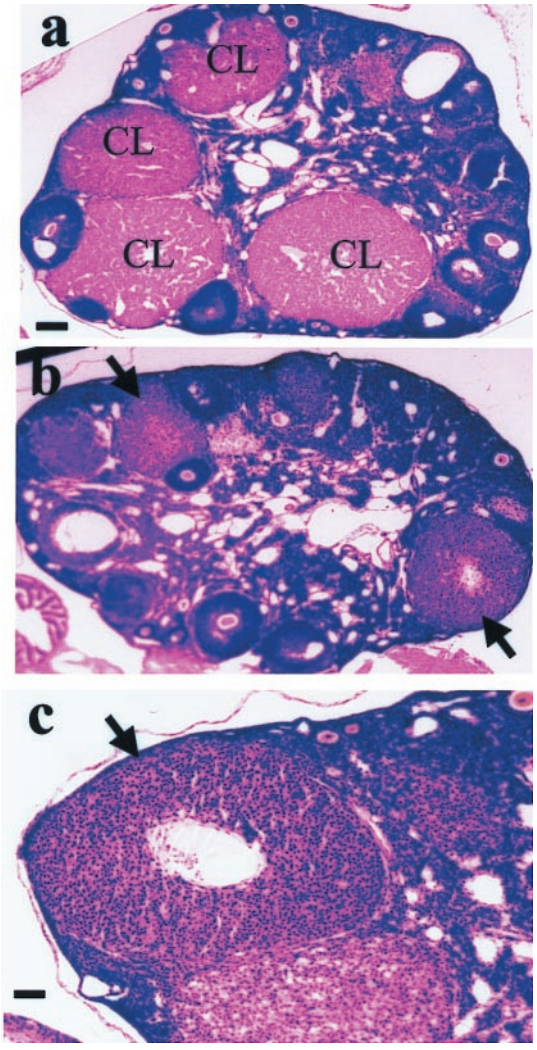

Fig. 6. Abnormal development of follicles in $CCS^{-/-}$ mice. Histological analysis of ovaries from age-matched (*a*) $CCS^{+/+}$ or (*b* and *c*) $CCS^{-/-}$ mice. Several corpora lutea (CL) and follicles in different stages of development are observed in control mice in *a*. In contrast, instead of corpora lutea, abnormally developed follicles are frequently seen in ovaries of $CCS^{-/-}$ mice (arrows in *b* and *c*). Bar = 40 μm in *a* and 10 μm in *c*.

kidney, and liver (Fig. 3*c*); we confirmed the identity of SOD1 by protein-blotting analysis (Fig. 3*a*) and activity gel assay (Fig. 3*b*) of the same samples shown in Fig. 3*c*. In contrast, we failed to detect ^{64}Cu-labeled SOD1 in brain or spinal cord lysates from CCS-deficient mice, although low levels were detected in kidney or liver lysates (Fig. 3*c*). To examine the specificity of CCS, we monitored Cu incorporation into ceruloplasmin in the serum from these same CCS-deficient mice. As expected, although levels of ceruloplasmin remained constant (Fig. 3*d*), no differences in cellular Cu uptake or serum ceruloplasmin oxidase activity were observed in CCS-deficient mice as compared with control littermates (Fig. 3*d*). Cu incorporation into ceruloplasmin, however, was completely abolished in ceruloplasmin-deficient mice (Fig. 3*d*). Moreover, because we failed to observe any other pathological abnormalities in the $CCS^{-/-}$ mice (up to 8 mo of age) unrelated to deficiency in SOD1 activity (see below), including Cu uptake and distribution and incorporation into cuproenzymes (data not shown), we concluded that CCS is not essential for other aspects of copper incorporation.

Similar results were observed when fibroblast cells derived from $CCS^{-/-}$ mice were metabolically labeled with ^{64}Cu. As expected, cultured fibroblasts derived from $CCS^{+/-}$ mice showed ≈50% reduction in level of CCS as compared with that of controls, whereas CCS was absent in fibroblasts derived from $CCS^{-/-}$ mice (data not shown). Furthermore, although the levels of SOD1 remained constant in control, $CCS^{+/-}$ and $CCS^{-/-}$ fibroblasts (Fig. 4*a*), no SOD1 activity was detected in $CCS^{-/-}$ fibroblasts (Fig. 4*b*). Significantly, although control or $CCS^{+/-}$ cells showed ^{64}Cu incorporation into SOD1, no ^{64}Cu-SOD1 was detected in $CCS^{-/-}$ fibroblasts (Fig. 4*c*). Taken together, these results demonstrate that CCS is essential to incorporate Cu into SOD1 to activate the enzyme in mammalian cells.

Increased Sensitivity to Paraquat and Reduced Fertility in $CCS^{-/-}$ Mice. Previous studies documented that SOD1-deficient mice are hypersensitive to axonal injury (19) and to paraquat exposure (20, 21), and female $SOD1^{-/-}$ mice exhibit reduced fertility (21, 22). To further demonstrate the loss of SOD1 activity observed in $CCS^{-/-}$ mice, we tested the possibilities that there is increased sensitivity to paraquat and reduced fertility in $CCS^{-/-}$ mice. Intraperitoneal administration of paraquat (15 mg/kg body weight) had a dramatic effect on CCS-deficient mice: after exposure, ≈60% of these mice were killed; the average survival time was 5 days (Fig. 5*a*). With a higher dose of paraquat (25 mg/kg body weight) at which ≈90% of control mice were unaffected, >90% of CCS-deficient mice were killed, with an average survival time of 4 days (Fig. 5*b*). Similar to $SOD1^{-/-}$ mice, $CCS^{-/-}$ mice were listless about 1 hr after the paraquat injection, whereas control littermates showed no overt phenotype. Examination of paraquat-treated $CCS^{-/-}$ mice revealed striking edema and hemorrhage in the lungs, features that are characteristic of paraquat toxicity (data not shown).

To assess female fertility, a breeding program for $CCS^{+/-}$ and $CCS^{-/-}$ mice was monitored. Mating of 4 heterozygous CCS females resulted in 8 litters with an average of 6.5 pups/litter over a period of 3 mo, whereas 4 homozygous CCS females gave 4 litters with an average of 3.5 pups/litter. These observations indicated that female $CCS^{-/-}$ mice exhibit reduced fertility, a phenotype that is characteristic of the SOD1-deficient mice (21, 22). To determine the reasons for this phenotype, we examined the ovaries of CCS-deficient mice at different ages. Compared with controls (Fig. 6*a*), ovaries from CCS-deficient mice (Fig. 6 *b* and *c*) possess fewer numbers of mature follicles and corpora lutea. Remarkably, abnormally developed follicles that are never seen in control ovaries are frequently observed in $CCS^{-/-}$ ovaries (Fig. 6 *b* and *c*). Taken together, our results establish that mammalian CCS is essential for *in vivo* Cu incorporation into SOD1 to efficiently activate this metalloenzyme.

Discussion

Copper chaperones are required for proper intracellular delivery of Cu so that Cu is incorporated into specific targets within different cellular compartments (2). Moreover, because it is believed that the cell possesses a high Cu chelating capacity, the level of intracellular free Cu is kept extraordinarily low, and the toxic effects of intracellular Cu are minimized (5). Given such restricted availability of intracellular free Cu, copper chaperones therefore function to sequester and deliver Cu to their respective protein targets. Although recent efforts showed that the yeast CCS (lys7) is necessary and sufficient to incorporate Cu into yeast SOD1 under a physiological level of free Cu (3, 5, 23), it was not known whether CCS is required to activate SOD1 in mammalian cells. Our results demonstrating that marked reductions of SOD1 activity in tissues of CCS-deficient mice is caused by impaired Cu incorporation into SOD1 now establish that CCS is essential for *in vivo* copper incorporation into SOD1 to activate the mammalian enzyme. Although the intracellular free Cu concentration in mammalian cells remains to be determined, our observations are consistent with the view that the copper

chaperone is essential to protect Cu for delivery to SOD1 under low levels of intracellular free Cu.

Despite our demonstration that CCS is essential for activation of SOD1, low levels of Cu incorporation into SOD1 observed in liver and kidney of $CCS^{-/-}$ mice raise the possibilities that intracellular free Cu concentration is sufficiently high for SOD1 to acquire Cu independent of CCS, and/or that the affinity of mammalian SOD1 for Cu is greater than that of yeast SOD1. However, our data do not exclude the possibility that there exists another mammalian CCS homologue that serves to incorporate Cu into SOD1. In view of the fact that SOD1 depends on yeast CCS for Cu incorporation under low concentrations of free Cu (5), low levels of Cu incorporation into SOD1 observed in $CCS^{-/-}$ mice within certain tissues or cell types suggest that in tissues where Cu availability is higher, SOD1 could acquire Cu independent of CCS. For example, we have shown that higher levels of Cu incorporation into SOD1 were observed in liver and kidney as compared with those seen in spinal cord, brain, or fibroblasts (Figs. 3 and 4). Our results imply that certain mammalian cell types such as fibroblasts may possess a greater intracellular Cu chelating capacity, similar to that seen in yeast, whereas others tolerate higher levels of intracellular free Cu concentration. However, the physiological significance of differences in Cu availability in different mammalian cell types remains to be established. The demonstration that the level of active SOD1 could be altered by either restricting or increasing Cu availability in cells deficient in CCS would further support the view that CCS is required to incorporate Cu into mammalian SOD1 to activate the enzyme only under low concentrations of intracellular free Cu (5).

Mutations in SOD1 cause ≈15% of cases of familial ALS (9, 10), and a variety of *in vivo* and *in vitro* studies (reviewed in ref. 11) have demonstrated that the mutant enzyme causes selective neuronal degeneration through a gain of toxic property rather than a loss of superoxide dismutase activity, consistent with FALS displaying an autosomal dominant pattern of inheritance. However, the molecular mechanisms whereby mutant SOD1 causes selective motor neuron death remain uncertain. One hypothesis is that the Cu bound to mutant SOD1 plays a key role in generating the toxic property in SOD1-linked FALS, i.e., mutations induce conformational changes in SOD1 to facilitate the interactions of the catalytic Cu with small molecules such as peroxynitrite (12) or hydrogen peroxide (24) to generate toxic free radicals that damage a variety of cell constituents important for the maintenance and survival of motor neurons. Consistent with this view are results showing increased levels of free nitrotyrosine in G37R mutant SOD1 transgenic mice (25) and in both sporadic and familial ALS (26, 27), as well as the demonstration that the glutamate transporter, GLT1, is inactivated by oxidative reactions initiated by hydrogen peroxide and catalyzed by FALS-linked mutant SOD1 (28). However, no experimental proof for these aberrant Cu chemistries, proposed to be central to the pathogenesis of FALS, has yet been established.

The discovery of CCS (3) provides the opportunity to test whether Cu within mutant SOD1 mediates motor neuron degeneration in SOD1-linked FALS. Recent studies showed that one common property of both wild-type and FALS-linked mutant SOD1 is that Cu incorporation is CCS dependent. Thus, with regard to mutant SOD1, aberrant Cu chemistry may mediate degeneration of motor neurons in FALS (23). Consistent with this view are findings that CCS physically interacts with SOD1 (4, 5) and that both proteins are colocalized in many cell types, including motor neurons (6). Our demonstration that $CCS^{-/-}$ mice are viable and possess marked reductions in SOD1 activity now offers an opportunity to test directly whether Cu in mutant SOD1 plays a key role in the pathogenesis of mutant SOD1-induced FALS. Outcomes of crossbreeding strategies by using these $CCS^{-/-}$ mice and FALS-linked mutant SOD1 mice (17, 29–31) should be instructive in deciphering the role of Cu in FALS. Results of these efforts, which will have the potential to identify novel therapeutic targets (i.e., CCS, SOD1, Cu trafficking pathways), may have important implications for design of drug treatments for FALS.

We thank D. Borchelt and A. Lawler for helpful discussions, H. Chen and S. Onda for support in molecular biological analysis, E. Southon for help with tissue culture, S. Reid for help with blastocyst injections, and G. Cristostomo for support in histology. This work has been supported by National Institutes of Health grants NS37771 (P.C.W.), NS37145 (D.L.P.), DK44464 (J.D.G.), GM50016 (V.C.C.), and by the Amyotrophic Lateral Sclerosis Association (P.C.W.). J.D.G. is the recipient of a Burroughs Wellcome Scholar Award in Experimental Therapeutics.

1. Valentine, J. S. & Gralla, E. B. (1997) *Science* **278,** 817–818.
2. Culotta, V. C., Lin, S. J., Schmidt, P., Klomp, L. W., Casareno, R. L. & Gitlin, J. (1999) *Adv. Exp. Med. Biol.* **448,** 247–254.
3. Culotta, V. C., Klomp, L. W. J., Strain, J., Casareno, R. L. B., Krems, B. & Gitlin, G. D. (1997) *J. Biol. Chem.* **272,** 23469–23472.
4. Casareno, R. L. B., Waggoner, D. & Gitlin, J. D. (1998) *J. Biol. Chem.* **273,** 23625–23628.
5. Rae, T. D., Schmidt, P. J., Pufahl, R. A., Culotta, V. C. & O'Halloran, T. V. (1999) *Science* **284,** 805–808.
6. Rothstein, J. D., Dykes-Hoberg, M., Corson, L. B., Becher, M., Cleveland, D. W., Price, D. L., Culotta, V. C. & Wong, P. C. (1998) *J. Neurochem.* **72,** 422–429.
7. Schmidt, P. J., Rae, T. D., Pufahl, R. A., Hamma, T., Strain, J., O'Halloran, T. V. & Culotta, V. C. (1999) *J. Biol. Chem.* **274,** 23719–23725.
8. Lamb, A. L., Wernimont, A. K., Pufahl, R. A., Culotta, V. C., O'Halloran, T. V. & Rosenzweig, A. C. (1999) *Nat. Struct. Biol.* **6,** 724–729.
9. Rosen, D. R., Siddique, T., Patterson, D., Figlewicz, D. A., Sapp, P., Hentati, A., Donaldson, D., Goto, J., O'Regan, J. P., Deng, H.-X., *et al.* (1993) *Nature (London)* **362,** 59–62.
10. Deng, H.-X., Hentati, A., Tainer, J. A., Iqbal, Z., Cayabyab, A., Hung, W.-Y., Getzoff, E. D., Hu, P., Herzfeldt, B., Roos, R. P., *et al.* (1993) *Science* **261,** 1047–1051.
11. Wong, P. C., Rothstein, J. D. & Price, D. L. (1998) *Curr. Opin. Neurobiol.* **8,** 791–799.
12. Beckman, J. S., Carson, M., Smith, C. D. & Koppenol, W. H. (1993) *Nature (London)* **364,** 584.
13. Wong, P. C., Zheng, H., Chen, H., Becher, M. W., Sirinathsinghji, D. J. S., Trumbauer, M. E., Chen, H. Y., Price, D. L., Van der Ploeg, L. H. T. & Sisodia, S. S. (1997) *Nature (London)* **387,** 288–292.
14. Mansour, S. L., Thomas, K. R. & Capecchi, M. R. (1988) *Nature (London)* **336,** 348–352.
15. Swiatek, P. J. & Gridley, T. (1993) *Genes Dev.* **7,** 2071–2084.
16. Pardo, C. A., Xu, Z., Borchelt, D. R., Price, D. L., Sisodia, S. S. & Cleveland, D. W. (1995) *Proc. Natl. Acad. Sci. USA* **92,** 954–958.
17. Wong, P. C., Pardo, C. A., Borchelt, D. R., Lee, M. K., Copeland, N. G., Jenkins, N. A., Sisodia, S. S., Cleveland, D. W. & Price, D. L. (1995) *Neuron* **14,** 1105–1116.
18. Crapo, J. D., McCord, J. M. & Fridovich, I. (1978) *Methods Enzymol.* **53,** 382–393.
19. Reaume, A. G., Elliott, J. L., Hoffman, E. K., Kowall, N. W., Ferrante, R. J., Siwek, D. F., Wilcox, H. M., Flood, D. G., Beal, M. F., Brown, R. H., Jr., *et al.* (1996) *Nat. Genet.* **13,** 43–47.
20. Huang, T. T., Yasunami, M., Carlson, E. J., Gillespie, A. M., Reaume, A. G. & Hoffman, E. K. (1997) *Arch. Biochem. Biophys.* **344,** 424–432.
21. Ho, Y. S., Gargano, M., Cao, J., Bronson, R. T., Heimler, I. & Hutz, R. J. (1998) *J. Biol. Chem.* **273,** 7765–7769.
22. Matzuk, M. M., Dionne, L., Guo, Q., Kumar, T. R. & Lebovitz, R. M. (1998) *Endocrinology* **139,** 4008–4011.
23. Corson, L. B., Culotta, V. C. & Cleveland, D. W. (1998) *Proc. Natl. Acad. Sci. USA* **95,** 6361–6366.
24. Wiedau-Pazos, M., Goto, J. J., Rabizadeh, S., Gralla, E. B., Roe, J. A., Lee, M. K., Valentine, J. S. & Bredesen, D. E. (1996) *Science* **271,** 515–518.
25. Bruijn, L. I., Beal, M. F., Becher, M. W., Schulz, J. B., Wong, P. C., Price, D. L. & Cleveland, D. W. (1997) *Proc. Natl. Acad. Sci. USA* **94,** 7606–7611.
26. Ferrante, R. J., Browne, S. E., Shinobu, L. A., Bowling, A. C., Baik, M. J., Macgarvey, U., Kowall, N. W., Brown, R. H., Jr. & Beal, M. F. (1997) *J. Neurochem.* **69,** 2064–2074.
27. Beal, M. F., Ferrante, R. J., Browne, S. E., Matthews, R. T., Kowall, N. W. & Brown, R. H., Jr. (1997) *Ann. Neurol.* **42,** 646–654.
28. Trotti, D., Rolfs, A., Danbolt, N. C., Brown, R. H. & Hediger, M. A. (1999) *Nat. Neurosci.* **2,** 427–433.
29. Gurney, M. E., Pu, H., Chiu, A. Y., Dal Canto, M. C., Polchow, C. Y., Alexander, D. D., Caliendo, J., Hentati, A., Kwon, Y. W., Deng, H.-X., *et al.* (1994) *Science* **264,** 1772–1775.
30. Ripps, M. E., Huntley, G. W., Hof, P. R., Morrison, J. H. & Gordon, J. W. (1995) *Proc. Natl. Acad. Sci. USA* **92,** 689–693.
31. Bruijn, L. I., Becher, M. W., Lee, M. K., Anderson, K. L., Jenkins, N. A., Copeland, N. G., Sisodia, S. S., Rothstein, J. D., Borchelt, D. R., Price, D. L., *et al.* (1997) *Neuron* **18,** 327–338.